

Evidence of strong effects of the ^{11}Be halo structure on reaction processes at energies around the Coulomb barrier.

A.Di Pietro¹, F.Amorini^{1,2}, P.Figuera¹, M.Fisichella^{1,2}, M.Lattuada^{1,2}, A.Musumarra^{1,8}, M.Papa¹, M.G.Pellegriti^{1,2}, G.Randisi^{1,2,11}, F.Rizzo^{1,2}, D.Santonocito¹, G.Scalia^{1,2}, V.Scuderi^{1,2}, E. Strano^{1,2}, D.Torresi^{1,2}, L.Acosta³, I.Martel³, F.Perez-Bernal³, M.J.G.Borge⁴, A.Maira Vidal⁴, O.Tengblad⁴, L.M.Fraile^{5,12}, H.Jeppesen^{5,13}, D. Voulot⁵, F. Wenander⁵, J.Gomez-Camacho⁶, M.Milin⁷, R.Raabe⁹, M.Zadro¹⁰

¹INFN-Laboratori Nazionali del Sud and Sezione di Catania, Italy

²Dipartimento di Fisica ed Astronomia Università di Catania, Catania, Italy

³Departamento de Física Aplicada Universidad de Huelva, Huelva, Spain

⁴Instituto de Estructura de la Materia CSIC, Madrid, Spain

⁵ISOLDE, CERN, CH-1211 Geneva 23, Switzerland

⁶Departamento de Física Atomica Molecular Nuclear Universidad de Sevilla, and Centro Nacional de Aceleradores, Sevilla, Spain

⁷Department of Physics Faculty of Science University of Zagreb, Zagreb, Croatia

⁸Dipartimento di Metodologie Fisiche e Chimiche per l'Ingegneria Università di Catania, Catania, Italy

⁹Instituut voor Kern-en Stralingsfysica K.U.Leuven, Belgium

¹⁰Division of Experimental Physics Rudjer Bošković Institute, Zagreb, Croatia

E-mail: dipietro@lns.infn.it

Abstract. The collision induced by the three Beryllium isotopes, $^{9,10,11}\text{Be}$, on ^{64}Zn target were investigated at $E_{c.m.} \approx 1.4$ the Coulomb barrier. Elastic scattering angular distributions were measured for the $^{9,10}\text{Be}$ collisions whereas, in the ^{11}Be case the quasielastic scattering angular distribution was obtained. A strong damping of the quasielastic cross-section was observed in the ^{11}Be case, especially in the angular range around the Coulomb-nuclear interference peak. In this latter case a large total-reaction cross-section is found, more than a factor of two larger than the ones extracted in the reactions induced by the non-halo Beryllium isotopes. A large contribution to the total-reaction cross-section in the ^{11}Be case could be attributed to transfer and/or break-up events.

¹¹ present address: LPC-ENSICAEN, IN2P3-CNRS and Université de Caen, France

¹² present address: Departamento de Física Atomica, Molecular y Nuclear, Universidad Complutense, Madrid, Spain

¹³ present address: Nuclear Science Division, Lawrence Berkeley National Laboratory, Berkeley, USA

1. Introduction

The existence of a halo is a threshold phenomenon in which the 'halo' nucleons quantum tunnel out to large distances from the core, giving rise to a wave function having a tail extending mostly outside the potential well. Since elastic scattering is a peripheral process, it can be used as a tool to probe the tail of the wave function. Therefore, using elastic scattering one can investigate the surface properties of the halo nuclei. In this contribution we investigate to what extent information can be gained from high quality elastic scattering measurements at low bombarding energies. Low energy elastic scattering experiments, involving halo nuclei, have mostly been performed with the 2n-halo ${}^6\text{He}$ nucleus on several targets over a wide range of masses. The reason for that lies in the fact that a ${}^6\text{He}$ beam was available as post-accelerated beam in facilities like the CRC at Louvain la Neuve or GANIL. Reaction studies performed with ${}^6\text{He}$ have shown that coupling to the continuum (break-up), strongly affects the elastic cross-section. On heavy targets, as for example ${}^{208}\text{Pb}$, the coupling with the Coulomb dipole excitation of the low-lying E1 strength, produces a suppression of the elastic scattering angular distribution at forward angles, in the Coulomb-nuclear interference region [5]. This suppression has not been observed in reaction induced on low charge targets as ${}^{64}\text{Zn}$ [6]. On this target, however, the elastic cross-section is overall suppressed when compared for example to the elastic scattering angular distribution induced by the well bound ${}^4\text{He}$ at the same $E_{\text{c.m.}}$ [6]. Moreover, in the ${}^6\text{He}$ induced reactions the total-reaction cross-section is large (see e.g. [6, 7]). At low energies, near the Coulomb barrier, direct processes such as transfer and break-up are mostly contributing to the total-reaction cross-section. Exclusive measurements have shown that, among these processes, the 2n transfer gives the largest contribution [8, 9].

In the reaction induced by the 1n-halo ${}^{11}\text{Be}$ nucleus on a ${}^{209}\text{Bi}$ target at energy near the Coulomb barrier, the extracted total-reaction cross-section was found to be similar to the one of ${}^9\text{Be}+{}^{209}\text{Bi}$ [10, 11], measured by the same group [12]. Since the absorption is due to fusion (which for the two reactions ${}^{9,11}\text{Be}+{}^{209}\text{Bi}$ has a similar cross-section [13]) and break-up, the authors concluded that the breakup process must have similar cross-section in both ${}^{9,11}\text{Be}$ nuclei.

In this contribution new results of experiments performed with the three Beryllium isotopes ${}^{9,10,11}\text{Be}$ on a medium mass ${}^{64}\text{Zn}$ target will be discussed.

2. Experimental set-up.

In order to study the three reactions ${}^{9,10,11}\text{Be}+{}^{64}\text{Zn}$, two separate experiments were performed. The experiment with the stable ${}^9\text{Be}$ beam was done at Laboratori Nazionali del Sud (LNS) in Catania, whereas the experiment with the radioactive ${}^{10,11}\text{Be}$ beams was performed at REX-ISOLDE (CERN).

The ${}^9\text{Be}$ beam was impinging on a $550 \mu\text{g}/\text{cm}^2$ ${}^{64}\text{Zn}$ at a center of mass energy of 24.9 MeV. The elastic-scattering angular distribution was measured using five collimated surface barrier Si detector telescopes ($10 \mu\text{m}$ ΔE and $200 \mu\text{m}$ E detectors), placed on a rotating platform, in the angular range $10^\circ \leq \theta_{\text{c.m.}} \leq 150^\circ$.

In the ${}^{10,11}\text{Be}+{}^{64}\text{Zn}$ experiment the beam energy was $E_{\text{c.m.}}=24.5$ MeV for both beams and the target was a $550 \mu\text{g}/\text{cm}^2$ and a $1000 \mu\text{g}/\text{cm}^2$ for the ${}^{10}\text{Be}$ and ${}^{11}\text{Be}$ beams respectively. The detector system used was an array of six Si-detector-telescopes each formed by a $40 \mu\text{m}$, $50 \times 50 \text{ mm}^2$, ΔE DSSSD detector (16+16 strips) and a $1500 \mu\text{m}$ single pad E detector. This array was placed very close to the target; this allowed a large solid angle coverage. The angular range covered by the detector was $10^\circ \leq \theta_{\text{lab}} \leq 150^\circ$. More details on the experiment can be found in [1]. In the ${}^{11}\text{Be}$ case, due to the energy resolution of the radioactive beam and the energy straggling in the target, it was not possible to separate the ground state from the $\frac{1}{2}^-$ ($E_x=0.32\text{MeV}$) state in ${}^{11}\text{Be}$. As a consequence, in the ${}^{11}\text{Be}$ case, the quasielastic scattering rather than the elastic scattering was measured.

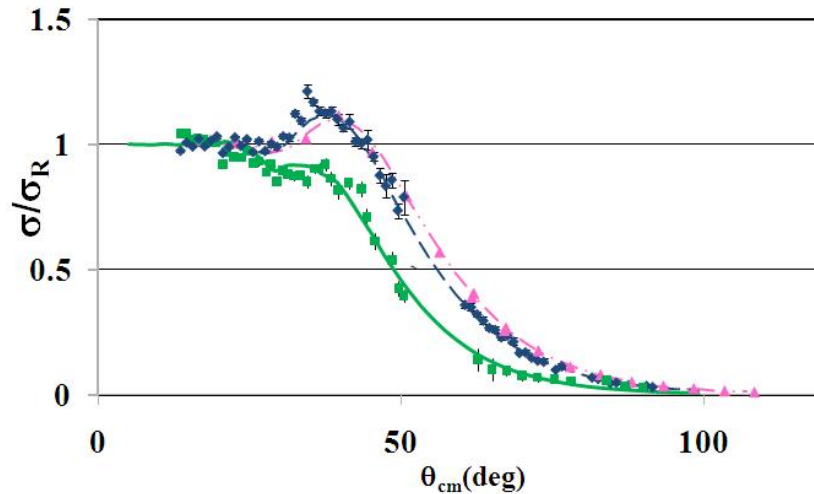


Figure 1. Elastic scattering angular distribution for ${}^9\text{Be}+{}^{64}\text{Zn}$ purple symbols and ${}^{10}\text{Be}+{}^{64}\text{Zn}$, blue symbols. Quasielastic angular distribution for ${}^{11}\text{Be}+{}^{64}\text{Zn}$, green symbols. Lines represent the result of the Optical Model fit to the data (see text for details).

3. Results and discussion

3.1. Elastic scattering angular distributions

The ${}^9\text{Be}$ is a stable weakly-bound nucleus ($S_n=1.67$ MeV), the ${}^{10}\text{Be}$ is radioactive but well bound ($S_n=6.81$ MeV) and it is the core of the ${}^{11}\text{Be}$ halo nucleus ($S_n=0.5$ MeV). In Fig. 1 a comparison of the extracted elastic scattering angular distribution for ${}^{9,10}\text{Be}+{}^{64}\text{Zn}$ and the quasielastic scattering angular distribution of ${}^{11}\text{Be}+{}^{64}\text{Zn}$ is shown. As one can see from the figure, the angular distributions for ${}^{9,10}\text{Be}+{}^{64}\text{Zn}$ appear to be very similar. This result is not surprising. It is known [2] that at energies above the Coulomb barrier the break-up of the weakly bound ${}^9\text{Be}$ does not give an important contribution to the total reaction cross-section. In fact, the total reaction cross-section in the ${}^9\text{Be}+{}^{64}\text{Zn}$ case is almost completely due to the total-fusion processes [2]. This result is similar to what expected in reactions induced by well bound nuclei such as ${}^{10}\text{Be}$. The ${}^{11}\text{Be}+{}^{64}\text{Zn}$ quasielastic angular distribution shows a very different behaviour; the peak due to the interference between the Coulomb and nuclear amplitude is missing and the quasielastic cross-section appear to be suppressed at the angles at which the nuclear interaction is felt. The observed feature of the ${}^{11}\text{Be}$ quasielastic angular distribution is typical of absorption occurring at large distances and it has been observed when a strong coupling with the Coulomb excitation of quadrupole states in heavy deformed nuclei is present due to the long-range of the Coulomb interaction [3]. In the ${}^{11}\text{Be}$ case, absorption at large distances may occur due to the large radial extension of the halo nucleus. As shown in [4], the suppression of the elastic cross-section in the Coulomb-nuclear interference region in the case of scattering of a halo nucleus with a low-charge target (as in the present study), at energies near the barrier, cannot be attributed to a strong Coulomb dipole coupling due to the presence of the low-lying E1 strength near the threshold. Such a strong coupling is expected to be important in the scattering with high charge targets, as observed in collisions induced by the 2n-halo ${}^6\text{He}$ nucleus see e.g. [5]. In the scattering of ${}^{11}\text{Be}$, investigated in the present case, nuclear coupling effects must therefore be important.

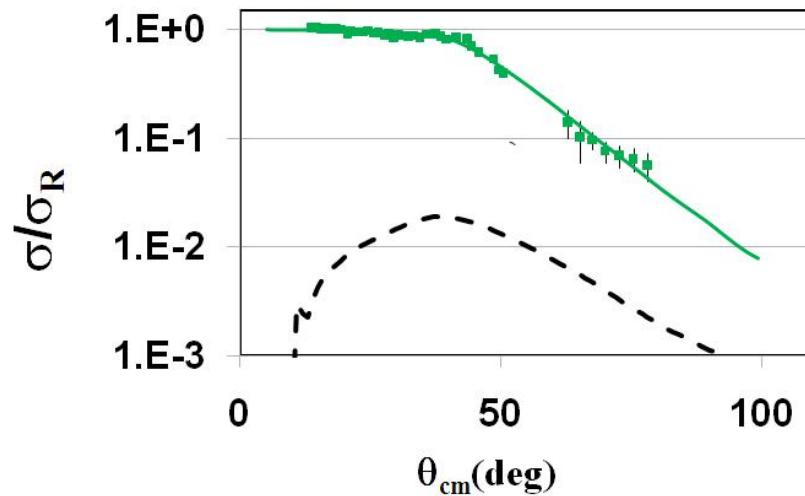


Figure 2. Quasielastic angular distribution for $^{11}\text{Be}+^{64}\text{Zn}$, green symbols. Full green line represent the result of the Optical Model fit to the data. Dashed black line represent DWBA calculations of inelastic scattering.

3.2. Optical Model analysis.

The $^{9,10,11}\text{Be}+^{64}\text{Zn}$ scattering was analyzed using the Optical Model (OM). For the $^{9,10}\text{Be}+^{64}\text{Zn}$ elastic scattering, a volume potential having a Woods-Saxon (W-S) shape for both the real and imaginary part was used; the radius and diffuseness (real and imaginary) were fixed and the best χ^2 was obtained by varying the potential depths. Before fixing radius and diffuseness, calculation were performed where they were varied at steps of 0.05 fm. The fit was done using the code PTOLEMY [14].

In the case of the $^{11}\text{Be}+^{64}\text{Zn}$ quasielastic angular distribution, the coupling to the break-up was taken into consideration using a Dynamic Polarization Potential (DPP). The DPP used was an imaginary surface potential having the shape of a W-S derivative. No real part for the DPP potential was considered. The volume potential responsible for the core-target interaction, was the one extracted from the $^{10}\text{Be}+^{64}\text{Zn}$ elastic scattering fit. The OM fit was performed using as free parameter the depth of the DPP potential and varying the diffuseness at steps of 0.05 fm. The best χ^2 were obtained for a DPP diffuseness parameter of $a_{\text{si}} \approx 3.5$ fm. A similar diffuseness ($a_{\text{si}}=3.2$ fm) of the surface DPP potential was obtained by [15, 16]. The results are shown in Fig. 1. The values of the obtained potential parameters can be found in [1].

As above mentioned, in the $^{11}\text{Be}+^{64}\text{Zn}$ case, the inelastic excitation of the ^{11}Be at $E_x=0.32$ MeV could not be separated from the elastic peak and therefore the quasielastic scattering angular distribution was obtained. We have verified, by means of DWBA calculations, that the inelastic contribution to the quasielastic scattering angular distribution is small and hence the quasielastic angular distribution can be considered as elastic scattering angular distribution. This can be seen in Fig. 2. Details of the calculations can be find in [1]. The total-reaction cross-sections deduced from OM analysis for $^{9,10,11}\text{Be}+^{64}\text{Zn}$ are $\sigma_R=1090$ mb, $\sigma_R=1260$ mb and $\sigma_R=2730$ mb respectively.

3.3. Cross-section for direct reactions

The analysis of the $\Delta E\%E$ spectra in the $^{11}\text{Be}+^{64}\text{Zn}$ case shows events, next to the ^{11}Be quasi-elastic peak, consistent with ^{10}Be coming from 1n transfer or break-up processes, as can be seen

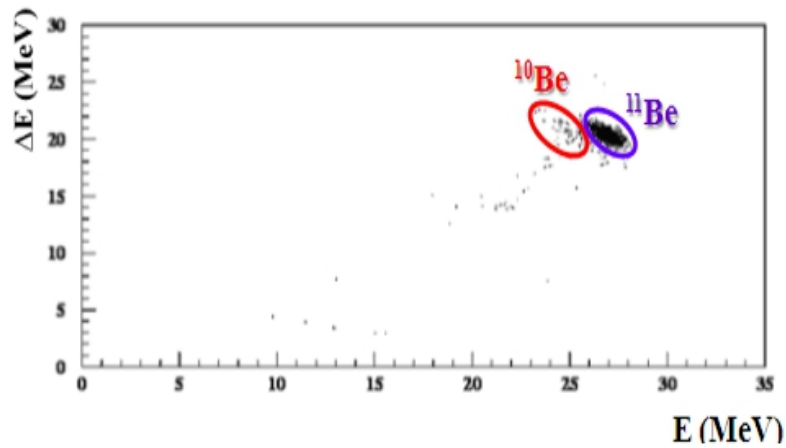


Figure 3. $\Delta E\%E$ scatter plot for the reaction $^{11}\text{Be}+^{64}\text{Zn}$.

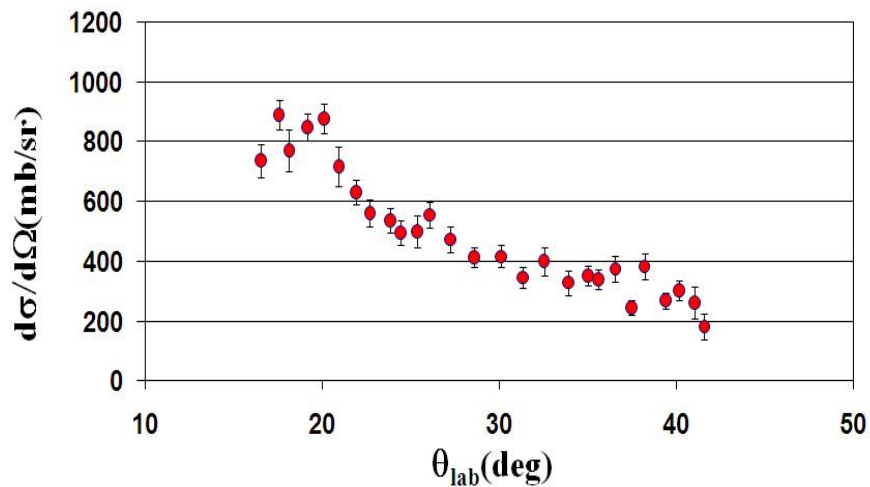


Figure 4. Angular distribution of transfer/break-up events in $^{11}\text{Be}+^{64}\text{Zn}$ obtained by selecting ^{10}Be events in the $\Delta E\%E$ spectrum.

in Fig. 3. For these events the angular distribution has been extracted and it is shown in Fig. 4. The integrated cross-section obtained from transfer/break-up angular distribution is $\sigma=1100 \pm 150$ mb, corresponding to $\approx 40\%$ of the extracted total-reaction cross-section. Therefore, contrary to what found in the weakly bound ^9Be case, where at a similar $E_{c.m.}$ energy the total-reaction cross-section is mainly due to fusion [2], in the ^{11}Be case direct processes are giving a large contribution to this cross-section.

4. Conclusions

The elastic and quasielastic scattering angular distribution has been measured for $^{9,10,11}\text{Be}+^{64}\text{Zn}$ and $^{11}\text{Be}+^{64}\text{Zn}$ respectively at $E_{\text{c.m.}} \approx 1.4$ the Coulomb barrier energy. A similar elastic-scattering angular distribution is observed for $^{9,10}\text{Be}+^{64}\text{Zn}$, which shows the typical Coulomb-nuclear interference peak. In the ^{11}Be quasielastic scattering instead this peak is strongly suppressed, showing that absorption occurs at much longer distances than for the other two Be isotopes [1]. An OM analysis was performed on the scattering data. In the $^{9,10}\text{Be}+^{64}\text{Zn}$ a W-S potential was used and only a volume potential was considered. However, in the ^{11}Be case, in order to take the coupling with the break-up into consideration, a surface DPP potential was considered in addition to the volume potential. The DPP used had the shape of a W-S derivative. The volume potential was extracted from the $^{10}\text{Be}+^{64}\text{Zn}$ elastic scattering OM fit. The best fit was obtained with the surface term having a very large diffuseness $a_{\text{si}} \approx 3.5$ fm in agreement with what found by [15, 16]. The total-reaction cross-section was extracted from the OM fit. A much larger cross-section is obtained in the ^{11}Be case. In the $^{11}\text{Be}+^{64}\text{Zn}$ experiment, ^{10}Be events coming from direct processes such as transfer and break-up, were identified. By measuring the angular distribution for such events it is found that they correspond to about 40% of the total-reaction cross-section. At the measured energy, above the Coulomb barrier, break-up processes do not play an important role in the weakly-bound ^9Be induced collision, where the total-reaction cross-section is found to be similar to the well bound ^{10}Be case. A behaviour of the elastic angular distribution similar to the one observed in the ^{11}Be case is found in collisions induced by the 2n-halo ^6He nucleus on heavy targets where coupling with the Coulomb dipole break-up is important. However, the large suppression of the elastic cross-section in the Coulomb-nuclear interference region has not been observed in the $^6\text{He}+^{64}\text{Zn}$ [6]. The larger radial distribution of the ^{11}Be compared to the ^6He [16] could be responsible for such a difference.

5. References

- [1] A. Di Pietro et al. *Phys. Rev. Lett.* **105**, 022701 (2010).
- [2] S.B. Moraes et al. *Phys. Rev. C* **61** (2000) 064608.
- [3] W.G. Love, T. Teresawa and G.R. Satchler *Nucl. Phys. A* **291** (1977) 183.
- [4] Y. Kucuk, I. Boztosun and N. Keeley *Phys. Rev. C* **79**, 067601 (2009).
- [5] A. M. Sánchez-Benítez et al. *Nucl. Phys. A* **803**, 30 (2008).
- [6] A. Di Pietro et al. *Phys. Rev. C* **69**, 044613 (2004).
- [7] E.F. Aguilera et al. *Phys. Rev. C* **63**, 061603R (2001).
- [8] A. Chatterjee et al. *Phys. Rev. Lett.* **101**, 032701 (2008).
- [9] P. A. DeYoung et al., *Phys. Rev. C* **71**, 051601(R) (2005).
- [10] M. Mazzocco et al., *Eur. Phys. J. A* **28**, 295 (2006)
- [11] M. Mazzocco et al., *Eur. Phys. J. S. T.* **150**, 37 (2007)
- [12] C. Signorini et al., *Nucl. Phys. A* **701**, 23c (2002)
- [13] P. A. DeYoung et al., *Eur. Phys. J. A* **2**, 27 (1998)
- [14] M.J. Rhoades-Brown et al. *Phys. Rev. C* **21**, 2417 (1980).
- [15] A. Bonaccorso and F. Carstoiu *Nucl. Phys. A* **706**, 322 (2002).
- [16] M. Hassan et al. *Phys. Rev. C* **79**, 064608 (2009).